

Enhancements to 3D preSDM salt-flank imaging

Ian F. Jones, Keith Ibbotson, Bill Henry, Andy Strachan, & Huibert Baud, CGG UK

Journal of Seismic Exploration: v7, No.3/4, December 1998, pp 329-346

Abstract

Here we present a technique for performing residual move-out correction of all CRP gathers output from the final iteration of a 3D pre-stack depth migration. We will show the effectiveness of this approach for improving the imaging of seismic events not explicitly described in the velocity-depth model, and for compensating for residual move-out resulting from small errors in the velocity-depth model. The results will be demonstrated on North Sea 3D pre-stack depth migrated data examples.

Introduction

Over the past few years, several authors have presented techniques for updating the velocity depth model required for performing full-volume 3D pre-stack depth migration (preSDM). With each technique, there are various theoretical or practical limitations. For example, the post-stack layer-stripping approach (Jones, 1993) presupposes that the velocities are known, and then updates the layer geometries. The Deregowski-loop (Deregowski, 1990) allocates a vertical 1D velocity estimate to an incorrect spatial location; the coherency scan ("inversion") technique supposes constant velocities within the 3D ray-bundle and only updates locally (Reshef, 1994); 3D tomographic inversion (Diet, et al., 1994) supposes a smooth model. More recently, the CRP-scan technique (Audebert & Diet, 1996; Jones et al, 1996) has been extended to a more generalised 3D inversion of perturbation values along the normals to the model surfaces so as to embed the updated velocity in the correct spatial location (Audebert, et al, 1997).

Regardless of the technique employed, the resulting CRP gathers will never be perfectly corrected for all events. Some degree of residual move-out will remain either because of failings in the velocity update technique, errors in picking, or compromises made in the model building. Amongst the typical compromises made are: picking on a coarse grid, editing 'anomalous' values, smoothing, or a limit on the number of layers maintained in the geophysical model (typically 10 or so). There will always be certain key events (perhaps in the reservoir interval with a low impedance contrast) which have not been included in the model building, and hence have not been 'constrained' to be flat in the CRP gathers. (Remember that it is only those horizons included in the model, that we are 'constraining' to become flat in the migrated CRP gathers).

The method

The basis of the technique is that described by Doicin et al (1995) wherein a CMP gather is NMO corrected, and then

a scan of perturbed residual NMO gathers is created from it. This ensemble of move-out corrected gathers is then input

to a coherency analysis routine to determine the 'best' move-out velocity on the basis of say, stack power. This approach results in an estimate of stacking velocity at each CMP location and each time sample. In this regard, their approach was not new, as similar techniques had been previously described (e.g. de Bazelaire, 1988). However, the important innovation in the work of Doicin et al., was related to the statistical analysis of the information produced so as to eliminate picks of peg-leg multiples, and to eliminate velocity information which showed little or no spatial (geological) coherence.

Here we describe an application of the technique of Doicin et al, adapted to the depth domain to effect a final residual depth-error correction to be applied to CRP gathers just prior to their being summed to form the final 3D preSDM image. This would presuppose that all model building had been done, and would constitute a fine-tuning of the CRP gathers.

The residual depth error or residual move-out correction has a very noticeable impact on data. We often find that although events in the CRP gathers associated with the main geological horizons in a pre-stack depth migrated data volume may be well flattened, the myriad of lesser intermediate events (not included explicitly in the velocity depth model) may contain residual move-out. With the technique presented here, a better image can be achieved by applying our automated residual depth error corrections to all CRP gathers just prior to forming the migrated image. Note however, that we need to output all the CRP gathers for the 3D preSDM volume in order to perform this correction.

It is stressed that this application in no way replaces the iterative model building effort necessary for successful completion of any preSDM project. It is merely designed to get the best possible image from the model so produced.

The most effective way to perform this correction is say to run the algorithm on lines 50m apart and then output the RMO correction velocity field. This is then checked, edited and smoothed prior to application to all CRP gathers.

Peg-leg multiple-velocity edition

One feature of the technique of Doicin is the suppression of velocities corresponding to peg-leg multiples. When the velocity table is being computed for a given CMP (with a numerical value of velocity for each time sample), each value is then assessed to see if it could correspond to a peg-leg multiple velocity. This is achieved by comparing the current velocity value with that which exists tau ms before it (where tau is the local water depth period). If the current velocity corresponds to a peg-leg multiple of a previous velocity, then the current value is deleted and replaced with

the velocity corresponding to the next-most energetic stack for this time.

Spatial continuity

Once the peg-leg multiple velocities have been removed from the table, a dip search is then conducted to see if the same numerical value of velocity persists on adjacent CMP's (within some dip range and velocity bounds). The length of the spatial coherence gate is a parameter of the process. Values which do not display spatial coherence are deleted from the table. The result of this stage of edition is the 'velocity skeleton'. The velocity skeleton resembles an auto-tracked horizon representation of the seismic section for this velocity line. We see horizons (or horizon segments) wherever we have spatially continuous velocity boundaries in the data.

Residual move-out correction

We emphasise that this RMO correction *in no way* replaces the model building phase of a project, but we assert that when all the model building is finished, we will still have events for which there will be some residual move-out. This is because:

1. there will always be some residual error in the velocity field
2. we may not have been able to resolve small-scale velocity anomalies (near faults)
3. smoothing required to meet the pre-requisites of travel time computation may result in some loss of velocity detail, eventually resulting in some residual move-out in the migrated gathers
4. for horizons not explicitly described in the model, the process of model building does not constrain the CRP gathers to be flat. Intermediate events may legitimately exhibit residual move-out.

In order to improve the image for these events, RMO is helpful. The process of automatic RMO works acceptably well on migrated data, as long as we take care not to correct multiples (either by visual QC of the RMO velocity field, and/or by application of the multiple eliminating option).

The overhead involved in this process is primarily that of needing to output all CRP gathers from the 3D survey, which makes the migration process longer due to the increased output required.

We will demonstrate the RMO procedure on four examples: in the first case the RMO has been completely automatic, but more generally, we advocate QC, editing and smoothing of this RMO velocity field prior to application, as done on the subsequent examples.

Salt Diapir example

In the first example the geological problem involves improved imaging of salt-flank sediments. These data (courtesy of Elf Norge) were initially part of a postSDM project, where the velocity model was built via iterative 3D tomographic inversion (TomCad®) in conjunction with

layer-stripping postSDM (Lanfranchi, et al, 1996, Jones, et al, 1995). Figure 1 shows a PetroCaem® 3D perspective view of the data with model horizons superimposed. These results were taken as the starting point for the preSDM work, to investigate the nature of improvements to be gained by 3D preSDM and application of RMO to the CRP gathers.

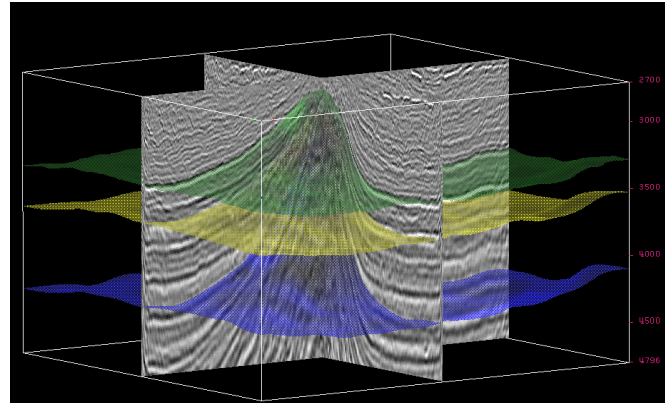


Figure 1: PetroCaem image of 3D salt dome

In figure 2, we see the 3D preSDM image for a line over the centre of the dome, and in figure 3, we see the 'velocity skeleton' of these salt dome data. Each 'point' in the skeleton corresponds to a location which displays lateral coherence in the velocity field. In this example, the length of the lateral coherence window was 19 CMP's. Hence, if we were to see an isolated value of velocity in this skeleton, it would tell us that there were only 19 consecutive CMP's which had approximately this velocity in the vicinity of this point (by 'vicinity' we mean within the dip search window on the segment being tracked).

A single line was chosen to demonstrate the details of the RMO process for this example: in figure 4 we see the RMS velocity profile from this line from the TomCad model, and figure 5 shows the corresponding RMS profile after RMO correction. An interpretation of the top-chalk event is superimposed to give some geological reference. It should be noted that at this stage, no model has been input to the process. The procedure is entirely automatic. It is only if we invert to interval velocities that a model is used.

In figure 6, we see some CRP gathers from the salt-flank data, resulting from 3D preSDM with the final model: the deeper events are not flattened (they were not explicitly described in the model). By comparison, the results after automatic RMO correction show that the hitherto non-flat events have been flattened (figure 7).

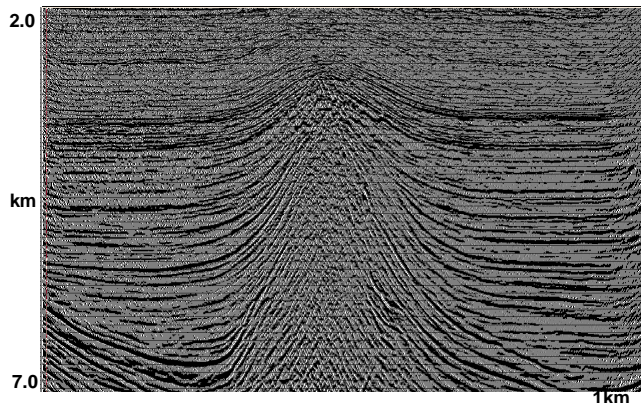


Figure 2: 3D preSDM image resulting from final TomCad model

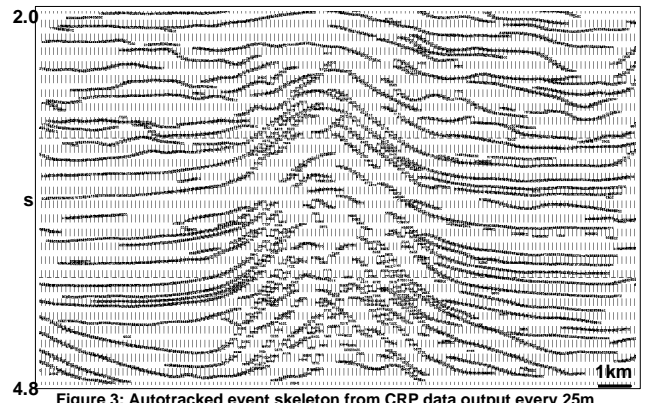


Figure 3: Autotracked event skeleton from CRP data output every 25m (19 point operator)

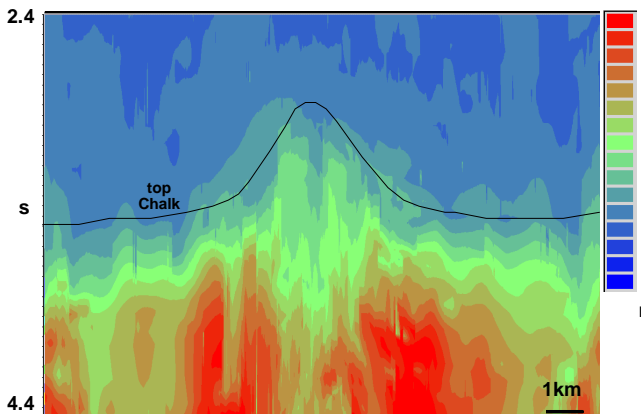


Figure 5: RMS velocity after RMO (25m CRP spacing, 19 point operator)

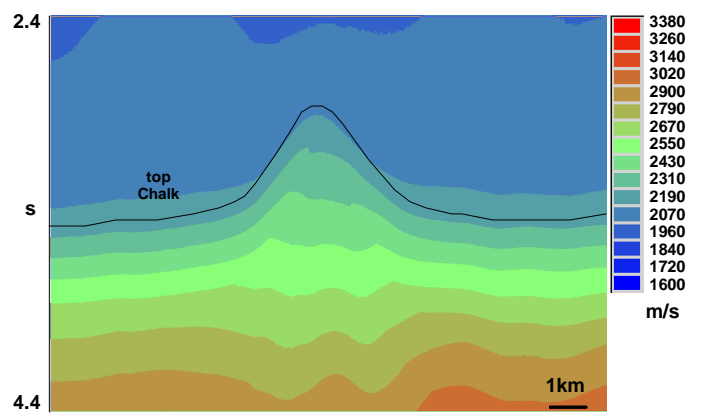


Figure 4: RMS velocity of preSDM model: 3D tomographic inversion on 200m grid

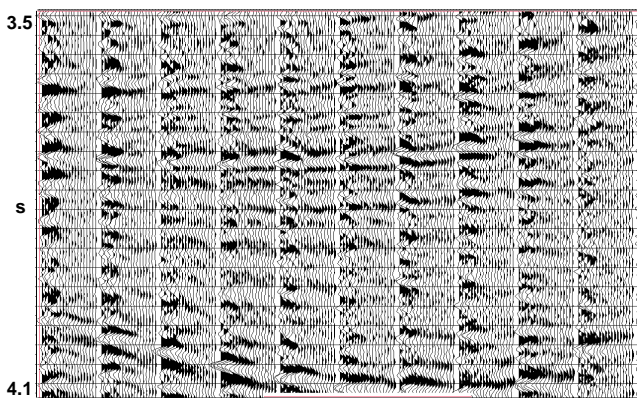


Figure 6: 3D preSDM CRP gathers on right flank of salt dome before RMO

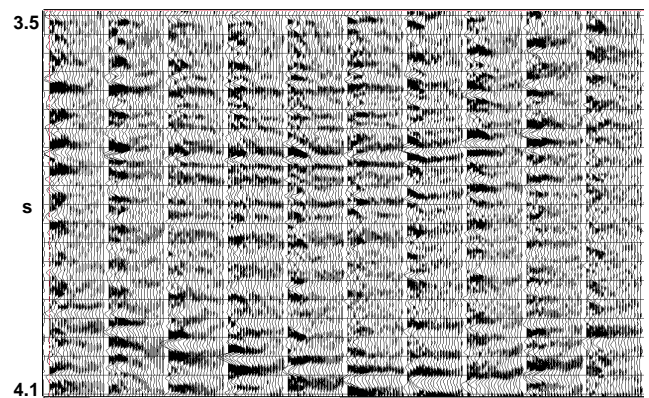


Figure 7: 3D preSDM CRP gathers on right flank of salt dome after RMO

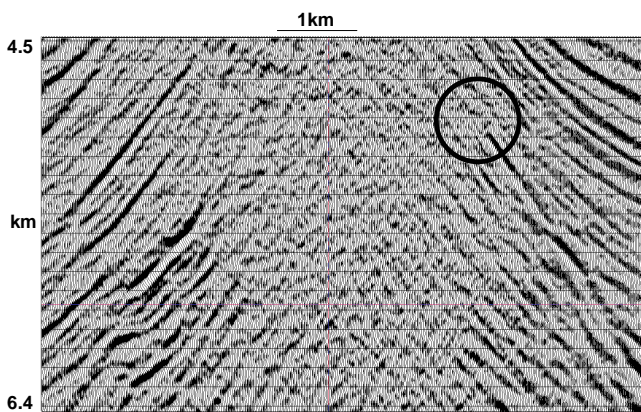


Figure 8: 3D preSDM image resulting from final TomCad salt-dome model

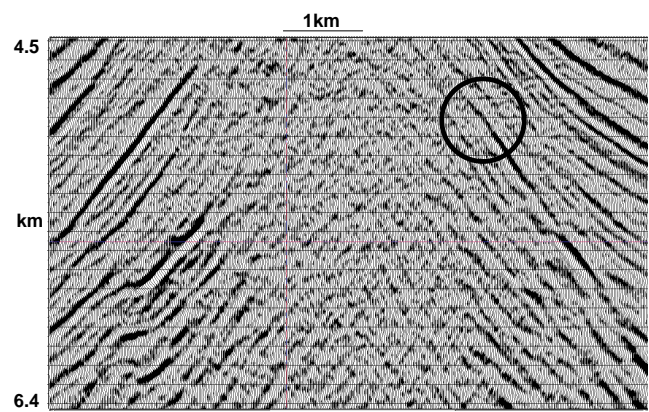


Figure 9: 3D preSDM image resulting from RMO corrected CRP gathers

In figure 8, the 3D preSDM image resulting from the TomCad model is shown: here we see a salt-flank image using the final velocity model. Most events in the CRP gathers were flat, but for horizons not explicitly described in the model, this is not guaranteed. On the steep event in the right centre of the figure, we see a termination at a depth of about 5km in the 3D preSDM result (circled). However, in the image produced by automatic RMO correction (figure 9), we see an extension of this event by some 200m, such that it now appears to terminate at a depth of 4800m (circled).

It is true to say that RMO will not correctly position the under or over corrected events in the CRP gathers, as it is clear that the preceding migration itself was in error. However, this is of secondary importance in this context... we have *finished* the model building, we are merely 'squeezing' the best possible image out of this migration. Also, for most cases, the degree of RMO will be small (hence the positioning error small)... but the degree of clarification in the image can still be large even for small RMO, due to the damaging effect of stacking even slightly misaligned events.

We quantify the relative benefit of RMO on stack response as opposed to mispositioning due to velocity error with a simple analytic example. For a 30Hz wavelet, on an event with a 30 degree dip, and interval velocity of 2km/s, for gathers with a 3km maximum offset we plot in figure 10 the loss of stack power (in dB) resulting from residual move-out (curve a). In the same figure, we plot lateral positioning error resulting from the velocity error corresponding to this residual move-out (curve b). Here, an RMO error of about 18m on the far trace of the CRP gather, corresponds to a lateral positioning error of 36m, but gives rise to 6dB loss in stack power.

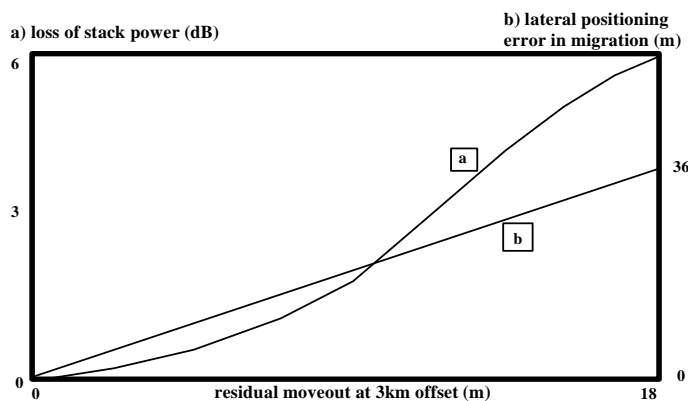


Figure 10: a relatively small residual moveout error results in a significant loss of stack power, even though it corresponds to a small migration positioning error

Gas cloud example

The second example of the RMO technique is taken from a gas cloud problem associated with another North Sea salt swell (courtesy of Kerr-McGee UK). In figure 11, we see a preSDM seismic section from this 3D survey, after the last iteration of CRP-scan model building (using the CRP-scan technique on a 300m by 300m grid). Using the continuous RMO technique on lines separated by 50m, sampled every

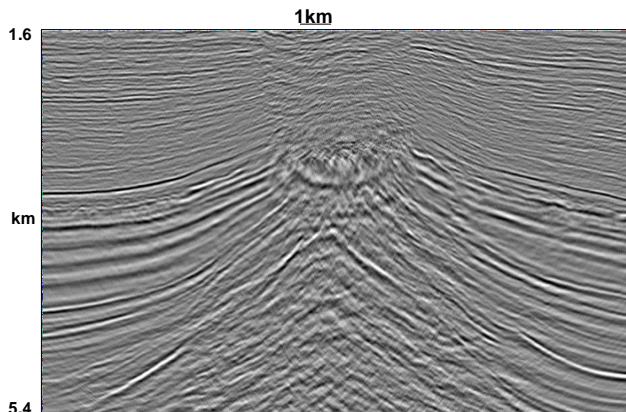


Figure 11: 3D preSDM image from final preSDM model

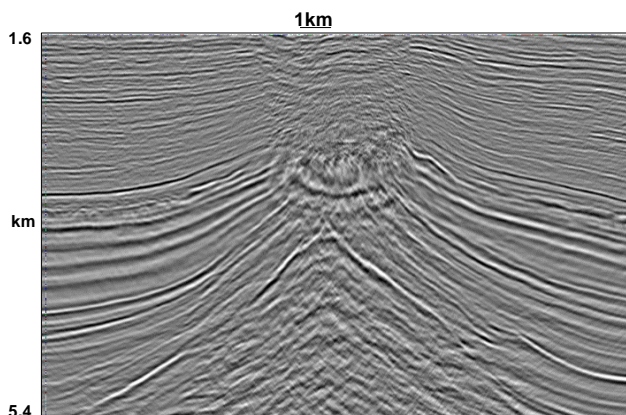


Figure 12: 3D preSDM image from final RMO'd gathers

25m along the lines, and after smoothing the resultant velocity field, we obtain the RMO corrected preSDM image (figure 12). In figures 13 & 14, we have the respective RMS velocity profiles for this line, before and after RMO. The percentage difference of these two velocity profiles shows the degree of RMO applied on this section (figure 15). We can use the percentage difference images as a guide to QC-ing the results (to ensure that we have not enhanced a multiple for example).

Faulted chalk/salt example

In this example (courtesy of Shell UK & Esso UK, described by Jones et al, 1996) a thick chalk layer, containing three velocity gradient regimes, is faulted with a vertical displacement of 1.5km. To the right of the fault, the chalk abuts salt intrusions. The zone of interest lies below the overhanging footwall of the fault. In figure 16 we see a PetroCaem® 3D perspective view showing the base chalk event outlined in red.

In figure 17 we see a comparison of some of the smaller-scale faulting, which is enhanced after application of RMO. We can see that the image of the small fault at 1.7s has been improved, and more importantly, the direction of the fault appears to have been unambiguously resolved.

Gas Basin example

In this final data example (courtesy of Amoco UK), we have salt movement on the Zechstein creating traps in the Rotliegendes sands. Clear imaging is imperative to accurately defining traps. In figures 18 & 19, we see an in-line section after 3D preSDM imaging before and after application of RMO.

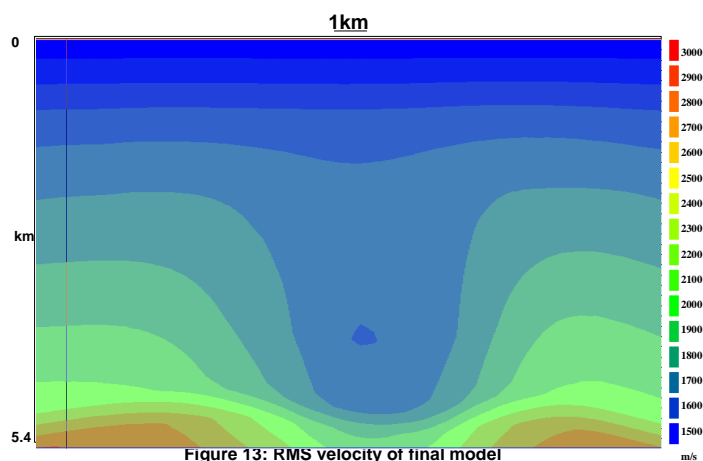


Figure 13: RMS velocity of final model

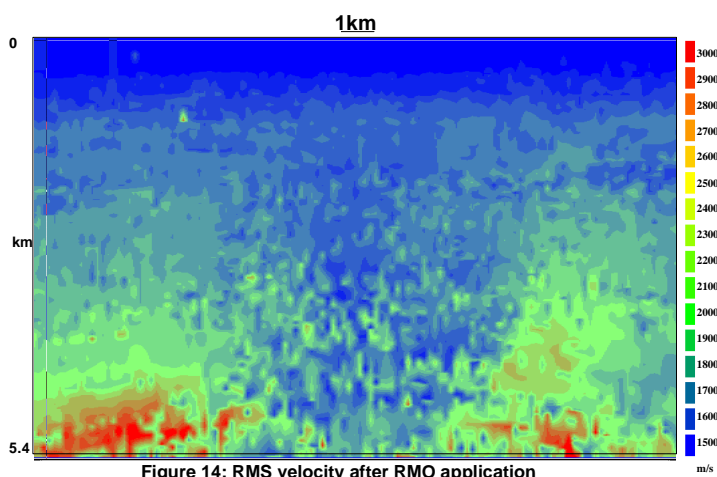


Figure 14: RMS velocity after RMO application

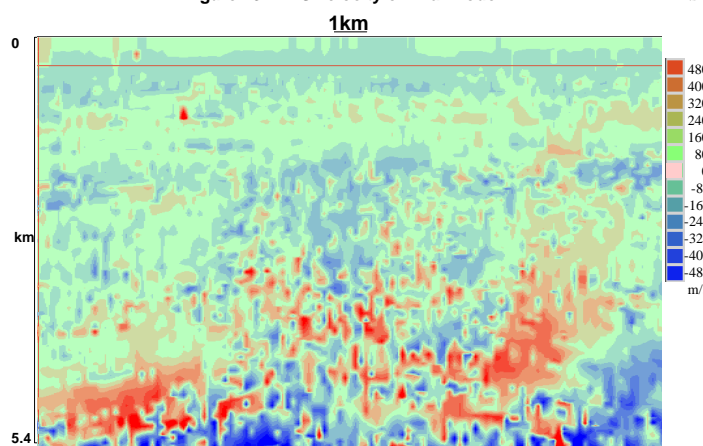


Figure 15: residual move-out error

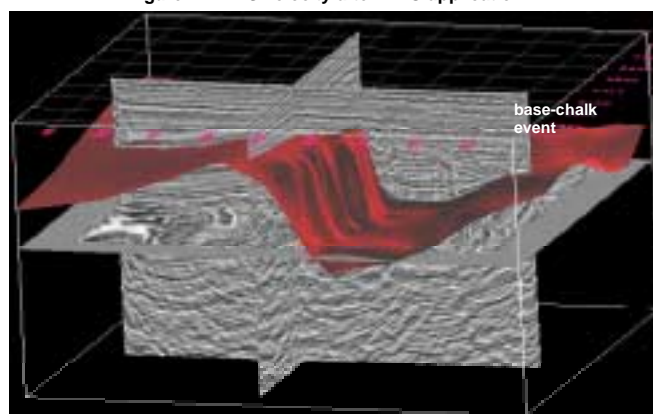


Figure 16: PetroCaem view of initial 3D postSDM

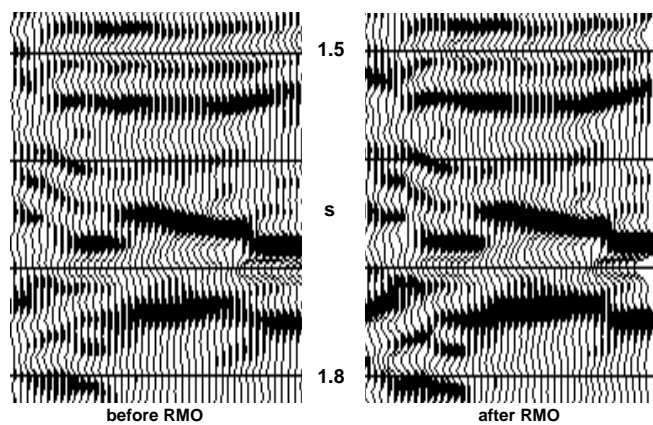


Figure 17: 3D preSDM image from faulted chalk data

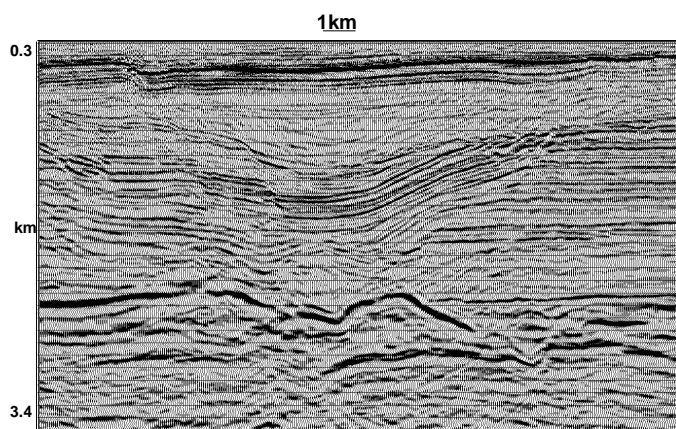


Figure 18: 3D preSDM image from final CRP gathers

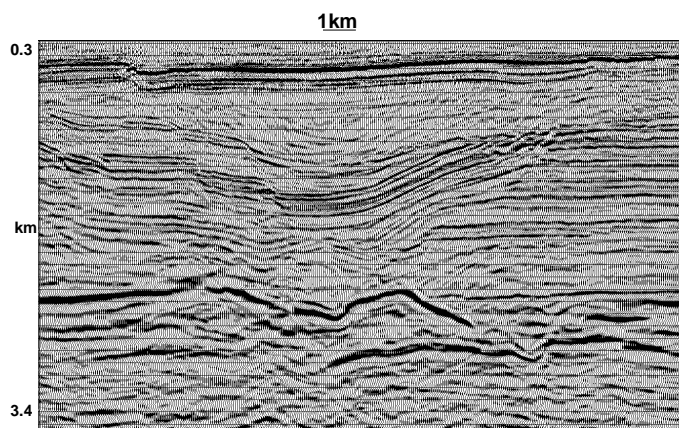


Figure 19: 3D preSDM image from final RMO'd gathers

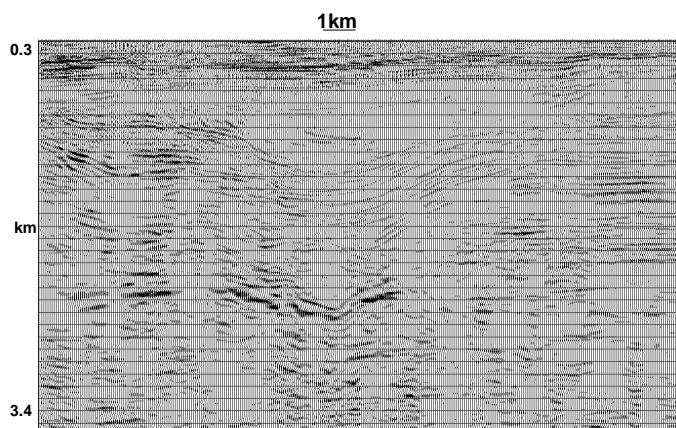


Figure 20: difference section between RMO and raw preSDM stacks

Enhancements to the lateral resolution and imaging quality are clearly visible in the RMO result. The difference between the raw CRP image and the RMO CRP image can be used as a QC product: we should always see an improvement in the RMO image when we have a significant difference (figure 20).

Conclusions

Once the process of iterative preSDM model building has been completed, the automated RMO analysis technique described here can be employed to offer significant improvements in stack response of the migrated CRP gathers. Even though the migration error is small for moderate RMO errors, the benefits to stacking of RMO correction are large.

We have demonstrated that RMO can improve the final image in an industrial application of 3D preSDM imaging. The RMO velocity field can be easily QC'd by investigating areas of maximal change, based on velocity difference plots, or seismic difference sections.

References

- Audebert, F, Guillaume,P. , Jones,I.F. , and Zhang, X, 1997. CRP-Scans: 3D PreSDM Migration Velocity Analysis via Zero-Offset Tomographic Inversion. Proceedings of the 1997 spring symposium of the Tulsa Geophysical Society, SEG.
- Audebert, F., Diet, J.P., 1996, CRP-scans from 3D pre-stack depth migration- a new tool for velocity model building, 58th Ann. Internat. Mtg. Europ. Assoc. Expl. Geophys.
- Diet, JP, Jones, I.F., Guillaume, P.,1994, A strategic approach to 3D pre-stack depth migration: 64rd Ann. Internat. Mtg. Soc. Expl. Geophys.
- de Bazelaire, E., 1988, Normal move-out revisited: inhomogeneous media and curved interfaces, Geophysics v53, p143.
- Deregowski, S., 1990, Common-offset migrations and velocity analysis, First Break, v8, No.6., 225-234.

- Doicin, D., Johnson, C., Hargreaves, N., and Perkins, C., 1995, Machine guided velocity interpretation, 57th Ann. Internat. Mtg. Europ. Assoc. Expl. Geophys.
- Jones, I.F., Audebert, F., Martin, S., & Ibbotson, K, 1997, Continuous 3D preSDM velocity analysis: 59th Ann. Internat. Mtg. Europ. Assoc. Expl. Geophys.
- Jones, I.F., Grimshaw, M., Ibbotson,K, & Jolley, B, 1996: A new technique for 3D preSDM model building: a North Sea case study, 58th Ann. Internat. Mtg. Europ. Assoc. Expl. Geophys.
- Jones, I.F., Diet, JP, Guillaume P., Audebert, F.,1995, A strategic approach to 3D pre-stack depth imaging: IN "Seismic Depth Estimation" Proceedings of the 1995 spring symposium of the Tulsa Geophysical Society, SEG.
- Jones, I.F., 1993, 3D velocity model building via iterative one-pass depth migration 63rd Ann. Internat. Mtg. Soc. Expl. Geophys. 974-977
- Lanfranchi, P., Langlo, L.T., Aamodt, A., Guillaume, P.,1996: Model building using 3D tomographic inversion of multi-arrivals- a North Sea case study, 58th Ann. Internat. Mtg. Europ. Assoc. Expl. Geophys.
- Reshef, M, 1994, The use of 3D pre-stack depth imaging to estimate layer velocities and reflector positions, EAEG/SEG summer workshop, construction of 3D macro velocity models

Acknowledgements

The authors wish to thank Amoco UK, Amerada Hess UK, British Gas, Conoco UK, Enterprise, Mobil UK; Shell UK and Esso UK; Elf Norge; and Kerr-McGee for their kind permission to use their respective data.

TomCad® is registered to CGG and Total. PetroCaem® is registered to CGG-Petrosystems.